Least Squares Retrieval of Microburst Winds from Single-Doppler Radar Data

CHONG-JIAN QIU*

Department of Atmospheric Science, Lanzhou University, People's Republic of China

QIN XU

Cooperative Institute for Mesoscale Meteorological Studies, University of Oklahoma, Norman, Oklahoma

(Manuscript received 21 February 1995, in final form 6 December 1995)

ABSTRACT

A least squares (LS) method is developed for retrieving low-altitude winds from single-Doppler radar scans. The method is tested with Denver airport microburst data and the results compared with the previously developed simple adjoint (SA) method. It is found that the LS method is slightly superior to the SA method for the microburst data obtained with fast radar scans ($\Delta\tau \approx 60$ s) but will become inferior to the SA method if the radar scans are twice as long ($\Delta\tau \approx 120$ s). Four previously developed detailed techniques for the SA method are used to improve the LS retrievals, and these include (i) using multiple-time-level data, (ii) imposing the weak divergence and weak vorticity constraints, (iii) retrieving the eddy coefficient and time-mean forcing term, and (iv) using the observed time-mean radial wind as a weak constraint. Because the control equation is used as a weak constraint in a finite-difference form, the LS method depends more on the smoothness constraints but is less sensitive to equation error and is computationally much more efficient than the SA method. An objective way for the selections of weights is also proposed and tested in this paper.

1. Introduction

Because the NEXRAD (Next Generation Weather Radar) network will provide only single-Doppler scanning over most areas in the United States, many methods for single-Doppler velocity retrievals and data assimilation have been developed in recent years (Sun et al. 1991; Kapitza 1991; Liou et al. 1991; Qiu and Xu 1992), and substantial progress has been made in demonstration of feasibility with real Doppler data (Tuttle and Foote 1990; Xu et al. 1994a,b; Sun and Crook 1994; Laroche and Zawadzki 1994; Shapiro et al. 1995). A review of the previously developed methods can be found in Qiu and Xu (1992), and this paper presents a new least squares (LS) method that is developed in parallel with the simple adjoint (SA) method of Xu et al. (1995).

The SA method was first developed by Qiu and Xu (1992) and then upgraded and tested with the Phoenix II data by Xu et al. (1994a,b) and further improved and tested with the Denver microburst data by Xu et al. (1995). As demonstrated in these studies, the SA method is "simple" since only the reflectivity conservation equation or radial-component momentum equation is used as the model's strong constraint, and the method is called "adjoint" since the adjoint technique is used to minimize the difference between the observed and model-predicted reflectivities or radial winds. The principle idea is to retrieve the time-mean winds by using a sequence of observations. By implementing this idea, the SA method cannot only eliminate the problems of nonuniqueness and/or singularity encountered by directly solving for the wind vector from only one or two model's equations, but it can also increase the accuracy and reduce the sensitivity of the retrieved winds to data errors. Clearly, the very same idea can be used with the LS method or other types of variational methods, and these types of extensions have been attempted and tested with Doppler data by several authors with varying degrees of success (Gal-Chen and Zhang 1993; Laroche and Zawadzki 1994; Shapiro et al. 1995). Since these authors developed their LS methods independently or, at least, not in parallel with the SA method, the relative advantages and disadvantages between the LS and SA methods were not examined. Although one may expect that the LS method will cost less CPU time (since only weak constraints are used) and can be more sensitive to data noise and temporal resolution (since the time derivative term in the cost function is computed directly from radar observations) than the SA method, these expected differences be-

* Additional affiliation: Cooperative Institute for Mesoscale Meteorological Studies, University of Oklahoma, Norman, Oklahoma.

Corresponding author address: Dr. Qin Xu, CIMMS/CAPS, University of Oklahoma, EC Room 1110, 100 E. Boyd, Norman, OK 73019-0628.

tween the two methods have not been quantified with real Doppler data. These problems are the topics of this paper. Moreover, several previously developed techniques for the SA method in Xu et al. (1994a,b) and Xu et al. (1995) may also improve the LS method. The related tests and numerical experiments will be performed in this paper.

In order to make close comparisons, the LS method developed in this paper will be tested with the same microburst data as in Xu et al. (1995). The LS method and related formulations are described in the next section. Numerical experiments are designed in section 3 to test the LS method with the previously developed techniques applied. The designed experiments are performed with the Denver microburst data, and the results are presented in section 4. By examining the sensitivities of the retrievals to the weights, an objective way for weight selections is proposed in section 5. Conclusions follow in section 6.

2. Description of the LS method

a. Model equation

When the radial wind is used as a "tracer" field, the radial momentum equation can be written into the following form in Cartesian coordinates (x, y, z) [see (3.1)–(3.2) of Xu et al. (1995)]:

$$\partial_t v_r + u_m \partial_x v_r + v_m \partial_y v_r - \kappa \nabla_H^2 v_r - F_m = F' \approx 0, \tag{2.1}$$

where $\mathbf{v} \equiv (u, v)$ is the horizontal wind vector, $v_r = (xu + yv)/r$ is the radial component wind, $v_\alpha = (xv - yu)/r$ is the tangential component wind, $r^2 \equiv x^2 + y^2$, ∇_H^2 is the horizontal Laplacian, and κ is the coefficient of horizontal eddy diffusion for radial velocity. Here $(\ )_m \equiv \tau^{-1} \int_0^\tau (\ )dt = N^{-1}\Sigma(\ )_n \Delta\tau$ denotes the time mean (or running mean) over the period $\tau \equiv N\Delta\tau$ that covers $N + 1$ sequential radar scans, $\Delta\tau$ is the time elapsed for one scan, the summation is for the total N time intervals (from $n = 1$ to $n = N$), and $(\ )_n$ denotes the mean value for the nth time interval. The horizontal vector wind $\mathbf{v} \equiv (u, v)$ is partitioned into a time-mean part $\mathbf{v}_m \equiv (u_m, v_m)$ and a temporal fluctuation part $\mathbf{v}' \equiv (u', v')$. The residual forcing term $F \equiv v_{\alpha m}^2/r - w\partial_z v_r - u'\partial_x v_r - v'\partial_y v_r + (2v_{\alpha m}v'_\alpha + v_\alpha'^2)/r - \partial_r p/\rho + \nu\partial_z^2 v_r$ is also partitioned into a time-mean part F_m and a temporal fluctuation part F', where w is the vertical velocity, p is the pressure, ρ is the density, and ν is the coefficient of vertical eddy diffusion for radial velocity. As explained in Xu et al. (1994a), (2.1) can be used as a constraint for the retrieval only if F' is neglected. Otherwise the total number of unknowns will be greater than the number of the discretized model equations plus the number of data points. However, the time-mean part of the unknown forcing can be retained and retrieved. The centrifugal term $v_{\alpha m}^2/r$ may not be very small but can be retrieved implicitly as a part of the time-mean forcing (as shown by Xu et al. 1994b).

b. Cost function

The objective here is to retrieve $(\mathbf{v}_m, F_m, \kappa)$ from the observed radial winds v_r by using (2.1) as a weak constraint (Sasaki 1970). The terms $\partial_t v_r$, $\partial_x v_r$, $\partial_y v_r$, and $\nabla_H^2 v_r$ in (2.1) can be directly computed from the observational data as long as the data are of sufficiently high resolution in space and time. The time-mean fields of $(\mathbf{v}_m, F_m)$ and constant κ can be determined by the least squares fitting of (2.1) to a sequence of the observed v_r fields over $N + 1$ time levels. The computation of $\partial_t v_r$ requires two time levels of data, so N linear algebraic equations can be obtained at each grid point. To be well posed, the number of equations cannot be smaller than the number of unknowns, and this requires $N > 2$ in our case. This requirement $(N > 2)$, however, does not guarantee that the derived linear algebraic equations are not ill conditioned. The retrievals will become very sensitive to data noise if the linear algebraic equations are ill conditioned. To prevent ill conditioning and suppress the noise, additional smoothness constraints need to be introduced. For this purpose, the Laplacian operator ∇_H^2 was used as a smoothing operator by Thacker (1988) and Laroche and Zawadzki (1994). For the microburst data used in Xu et al. (1995) and in this paper, the weak divergence and weak vorticity constraints are found more suitable and give better retrievals, while the Laplacian smoothing operator seems to cause too much smoothing and overly suppress the gradient and divergence in the microburst flow (not shown).

Based on the above considerations, the following cost function is used for the LS method:

$$J \equiv \frac{1}{2}\{\{P_1\Sigma(F')_n^2 + P_2\Delta_m^2 + P_3 d_m^2 + P_4\zeta_m^2\}\}, \tag{2.2}$$

where $\{\{(\ )\}\} \equiv \Omega^{-1}\iint (\ )d\Omega$ is the area-mean operator over the retrieval domain Ω (covered by the internal grid points); $(F')_n$ is the residual term in (2.1) averaged over the nth time interval [see (2.3)]; the summation Σ is from $n = 1$ to $n = N$ for the averaged residual terms over the N time intervals that cover the total $N + 1$ time levels; $\Delta_m \equiv v_{rm} - (v_{\text{rob}})_m$ is the difference between retrieved and observed time–mean radial velocities; $d_m \equiv \nabla_H \cdot \mathbf{v}_m$ is the retrieved time–mean divergence; and $\zeta_m \equiv \mathbf{k} \cdot \nabla_H \times \mathbf{v}_m$ is the retrieved time–mean vertical vorticity. The four weights P_1, P_2, P_3, and P_4 are given in the next subsection [see (3.1)]. The second term on the right-hand side of (2.2) imposes a weak constraint on the difference between retrieved and observed time-mean radial velocities. As in Xu et al. (1994b), this weak constraint is better than

strictly setting v_{rm} equal to the observed time-mean radial velocity. The residual term $(F')_n$ is computed by the following finite-difference scheme:

$$(F')_n = \frac{1}{\Delta\tau}(v_{rob,n+1} - v_{rob,n}) + \frac{1}{2}(u_m\partial_x + v_m\partial_y - \kappa\nabla_H^2) \times (v_{rob,n+1} + v_{rob,n}) - F_m, \quad (2.3)$$

where $v_{rob,n}$ denotes the observed radial velocities at the nth time level, the first-order spatial derivatives are computed by the standard fourth-order finite-difference scheme, and the Laplacian is computed by the standard second-order central finite-difference scheme. The time step is $\Delta\tau \approx 60$ s and the grid spacing is $\Delta x = \Delta y = 250$ m. They are the same as the temporal and spatial resolutions of the data.

c. Method of minimization

Two methods can be used to find the minimum of the cost function J in the space of $(\mathbf{v}_m, F_m, \kappa)$. The first method solves for $(\mathbf{v}_m, F_m, \kappa)$ from the Euler equation, which is a linear system of equations derived from the fact that the gradient of J with respect to $(\mathbf{v}_m, F_m, \kappa)$ should become zero at the minimum. This method is not suitable for our problem due to the large dimensions of $(\mathbf{v}_m, F_m, \kappa)$. The second method uses the standard conjugate-gradient algorithm (UMCGG in the IMSL Math/Library) to search for the minimum. This method uses iterative procedures but does not require large computer memories, and thus is suitable for our problem.

The conjugate-gradient algorithm requires the gradient of J with respect to $(\mathbf{v}_m, F_m, \kappa)$ computed at each iterative step, and explicit expressions for the gradient components can be derived by considering the following first-order variation of the cost function in (2.2):

$$\delta J \equiv \left\{\left\{P_1\Sigma(F')_n\left[(\delta u_m\partial_x + \delta v_m\partial_y - \delta\kappa\nabla_H^2)\frac{(v_{rob,n+1} + v_{rob,n})}{2} - \delta F_m\right]\right\}\right\} + \left\{\left\{P_2\frac{\Delta_m(x\delta u_m + y\delta v_m)}{r}\right\}\right\} - \{\{P_3(\delta u_m\partial_x d_m + \delta v_m\partial_y d_m)\}\} + \{\{P_4(\delta u_m\partial_y\zeta_m - \delta v_m\partial_x\zeta_m)\}\} + \{P_3 d_m\delta u_m\}_x + \{P_3 d_m\delta v_m\}_y - \{P_4\zeta_m\delta u_m\}_y + \{P_4\zeta_m\delta v_m\}_x, \quad (2.4)$$

where $\{\{(\ )\}\} \equiv \Omega^{-1}\iint(\ )d\Omega$ is the area-mean operator over the retrieval domain Ω (covered by the internal grid points), $\{(\ )\}_x \equiv \Omega^{-1}\int[(\ )|_{x_2} - (\ )|_{x_1}]dy$ is the difference between the line-integrals along the two lateral boundaries $x = x_2$ and $x = x_1$ of domain Ω, $\{(\ )\}_y \equiv \Omega^{-1}\int[(\ )|_{y_2} - (\ )|_{y_1}]dx$ is the difference between the line integrals along the two lateral boundaries $y = y_2$ and $y = y_1$ of domain Ω, and $(F')_n$ is the residual term computed by (2.3). Explicit expressions for the gradient components are derived from (2.4) as follows:

$$\frac{\partial J}{\partial u_m} = P_1\Sigma(F')_n\frac{\partial_x(v_{rob,n+1} + v_{rob,n})}{2} + P_2\frac{\Delta_m x}{r} - P_3\partial_x d_m + P_4\partial_y\zeta_m,$$

$$\frac{\partial J}{\partial v_m} = P_1\Sigma(F')_n\frac{\partial_y(v_{rob,n+1} + v_{rob,n})}{2} + P_2\frac{\Delta_m y}{r} - P_3\partial_y d_m - P_4\partial_x\zeta_m,$$

$$\frac{\partial J}{\partial F_m} = -P_1\Sigma(F')_n, \quad (2.5a)$$

for an internal grid point;

$$\frac{\partial J}{\partial u_m} = P_3 d_m \quad (\text{or } -P_3 d_m),$$

$$\frac{\partial J}{\partial v_m} = P_4\zeta_m \quad (\text{or } -P_4\zeta_m), \quad (2.5b)$$

for a grid point on the lateral boundary $x = x_2$ (or $x = x_1$);

$$\frac{\partial J}{\partial u_m} = -P_4\zeta_m \quad (\text{or } P_4\zeta_m),$$

$$\frac{\partial J}{\partial v_m} = P_3 d_m \quad (\text{or } -P_3 d_m), \quad (2.5c)$$

for a grid point on the lateral boundary $y = y_2$ (or $y = y_1$); and

$$\frac{\partial J}{\partial\kappa} = -\left\{\left\{P_1\Sigma(F')_n\frac{\nabla_H^2(v_{rob,n+1} + v_{rob,n})}{2}\right\}\right\}. \quad (2.5d)$$

The iterative procedure can start with a zero initial guess of $(\mathbf{v}_m, F_m, \kappa)$. The gradient components of J can be computed by using (2.5a)–(2.5d) with the initial guess, and then the conjugate-gradient algorithm

can be used to find a new estimate of $(\mathbf{v}_m, F_m, \kappa)$. The procedure can be iterated until J becomes nearly stationary in the vicinity of its minimum. Computationally, the iteration stops when the normalized (by the initial value of J) changes of the cost function in two consecutive steps of iteration is smaller than 10^{-6}; that is, when

$$\frac{(|J_k - J_{k-1}| + |J_{k+1} - J_k|)}{J_0} \leq 10^{-6}, \quad (2.6)$$

where J_k denotes the value of the cost function obtained at the kth step of iteration.

3. Data and experiment design

a. Data

In order to compare the LS method developed in this paper with the SA method, this study uses the same microburst data as in Xu et al. (1995). The data were collected by MIT Lincoln Laboratory on 11 July 1988 during the operational test and evaluation of the Terminal Doppler Weather Radar (TDWR) in Denver, Colorado, and descriptions of the weather condition and data preparation can be found in Elmore et al. (1990), Proctor and Bowles (1992), and Xu et al. (1995). The data contain 29 consecutive low-elevation scans taken at intervals of approximately 1-min and covering the period 2204–2233 UTC, and the gridded data have a 250-m resolution in Cartesian coordinates at the level of 190 m above the FL-2 radar and 317 m above UND radar. The portion (45 × 30) of the gridded data used in this study is shown by the inner rectangular domain in Fig. 1.

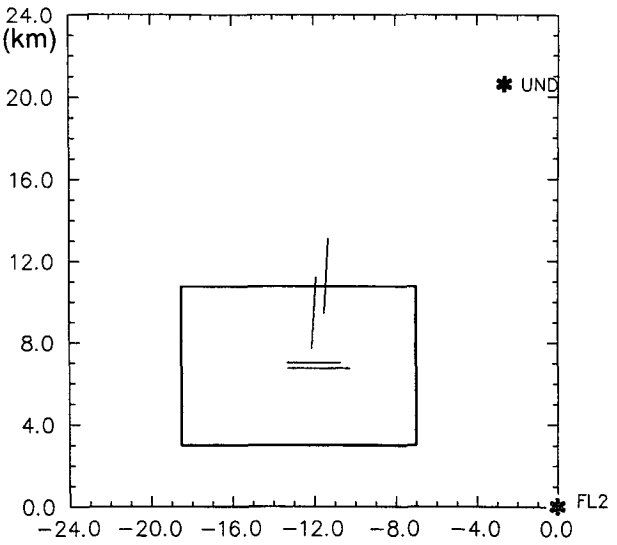

FIG. 1. Locations of airport runways (shown by lines) and radars (shown by asterisks). The FL-2 radar is at the origin and the UND radar is at (x, y) = (−2.717 km, 20.465 km) in the horizontal coordinate system as shown in the figure. The gridded data (with 250-m resolution) are given at the level of 190 m above the FL-2 radar and 317 m above UND radar. The portion (37 × 30) of the gridded data used in this study is shown by the inner rectangular domain (also see Figs. 2 and 3).

b. Selection of weights

In general the weights should be selected so that each of the penalty terms in the cost function would have the same order of magnitude. This implies that the four weights in (2.2) can be determined by $P_1 = \sigma_F^{-2}$, $P_2 = \sigma_v^{-2}$, $P_3 = \sigma_d^{-2}$, and $P_4 = \sigma_\zeta^{-2}$, where σ_F, σ_v, σ_d, and σ_ζ denote the root-mean-square (rms) amplitudes of $(F')_n$, Δ_m, d_m, and ζ_m, respectively. Since $\Delta_m \equiv v_{rm} - (v_{rob})_m$, σ_v can be related to the observational error in radial winds, and this yields a rough estimate of $\sigma_v = 0.2$ m s^{-1}. The residual term $(F')_n$ is affected by both the equation error and data error, and this makes it very difficult to accurately estimate σ_F from the observations. In this paper σ_F is assumed to be 0.1 of the rms amplitude of $\partial_t v_r$; that is, $0.1\{\{|\partial_t v_r|^2\}\}^{1/2}$, where the time derivative is estimated by $[v_{rob}(t + \tau) - v_{rob}(t)]\tau^{-1}$ for each retrieval period, so the estimated $P_1 = \sigma_F^{-2}$ is time dependent. Without a priori information of the true horizontal vector wind fields, it is difficult to accurately estimate σ_d and σ_ζ. In this paper the observed radial winds are projected onto the two coordinates of (x, y) to give a partial estimates of (u, v), and these partial estimated (u, v) are used to compute the partial divergence and vorticity. Then σ_d and σ_ζ are estimated by the rms amplitudes of the partial divergence and vorticity, respectively, computed for each radar over the entire grid and all the time levels. The estimated values are $\sigma_d = 4.18 \times 10^{-3}$ s^{-1} and $\sigma_\zeta = 2.76 \times 10^{-3}$ s^{-1} for the FL-2 radar data, and $\sigma_d = 3.16 \times 10^{-3}$ s^{-1} and $\sigma_\zeta = 2.56 \times 10^{-3}$ s^{-1} for the UND radar data. These estimated values are comparable with the values computed from the dual-Doppler data: $\sigma_d = 5.70 \times 10^{-3}$ s^{-1} and $\sigma_\zeta = 3.16 \times 10^{-3}$ s^{-1}. At least the ratio σ_d/σ_ζ is in the range between 1 and 2, as suggested by the dual-Doppler data. Based on the above consideration, the four weights are selected as follows:

$$P_1 = \sigma_F^{-2} = 100\left\{\left\{\left|\frac{[v_{rob}(t + \tau) - v_{rob}(t)]}{\tau}\right|^2\right\}\right\}^{-1},$$

$$P_2 = \sigma_v^{-2} = 25 \text{ m}^{-2} \text{ s}^2,$$

$$P_3 = \sigma_d^{-2} = 0.57 \times 10^5 \text{ s}^2 \quad \text{(FL-2 radar data)}$$

$$\text{or} \quad 1.0 \times 10^5 \text{ s}^2 \quad \text{(UND radar data)},$$

$$P_4 = \sigma_\zeta^{-2} = 1.3 \times 10^5 \text{ s}^2 \quad \text{(FL-2 radar data)}$$

$$\text{or} \quad 1.5 \times 10^5 \text{ s}^2 \quad \text{(UND radar data)}. \quad (3.1)$$

c. Experiment design

Six experiments are designed to test the LS method. Experiment 1 is the control experiment, in which the

weights are selected as in (3.1), and the time-mean forcing F_m and eddy coefficient κ are retrieved together with $\mathbf{v}_m$. This experiment performs 50 retrievals: 25 from the FL-2 radar data and 25 from the UND radar data. Each time-mean wind field is retrieved by using five consecutive time levels of data ($N = 5$), so the retrieving period is $\tau = (N - 1)\Delta\tau \approx 240$ s. Experiment 2 uses the same weights as experiment 1 but does not retrieve the time-mean forcing F_m. In this case, like the conventional LS method, the total forcing $F_m + F'$ is treated as a residual term of the governing equation. Experiment 3 sets $P_3 = P_4 = 0$, so it does not use the weak divergence and vorticity constraints. Experiment 4 uses only four time levels of data for each retrieval ($N = 4$ instead of $N = 5$), so the retrieving period is $\tau = (N - 1)\Delta\tau \approx 180$ s (instead of 240 s). Experiment 5 uses six time levels of data for each retrieval ($N = 6$), so the retrieving period is $\tau = (N - 1)\Delta\tau \approx 300$ s. Experiment 6 uses three time levels of data for each retrieval ($N = 3$) with the time interval doubled to $\Delta\tau \approx 120$ s, so the retrieving period ($\tau \approx 240$ s) remains the same as in experiment 1, but the temporal resolution of the input data is reduced. With this doubled time interval, this experiment performs 24 retrievals: 12 from the FL-2 radar data, and 12 from the UND radar data. Sensitivities of the retrievals to the weights will be examined in section 5.

The rms difference, the relative rms difference (RRD), and the spatial correlation coefficient (SCC) between the retrieved and dual-Doppler observed tangential winds are defined as follows:

$$\text{rms} \equiv \{\{|v_{\alpha m} - (v_{\alpha \text{ob}})_m|^2\}\}^{1/2}, \quad (3.2a)$$

$$\text{RRD} \equiv \frac{\text{rms}}{\{\{|(v_{\alpha \text{ob}})_m|^2\}\}^{1/2}}, \quad (3.2b)$$

$$\text{SCC} \equiv \frac{\{\{v'_{\alpha m}(v_{\alpha \text{ob}})'_m\}\}}{[\{\{|v'_{\alpha m}|^2\}\}\{\{|v_{\alpha \text{ob}})'_m|^2\}\}]^{1/2}}, \quad (3.2c)$$

where $(\ )' \equiv (\ ) - \{\{(\ )\}\}$. As the retrievals are weakly constrained by the observed time-mean radial winds [see the second term in (2.2)], the retrieved time-mean radial winds are very close to the observed time-mean radial winds and the averaged rms difference is only 0.4 m s^{-1}. After the retrievals are performed, the retrieved time-mean radial winds are replaced by the observed time-mean radial winds. In this case, the rms difference between the retrieved and dual-Doppler observed vector winds is the same as the rms difference for the tangential winds in (3.2a).

In the above six experiments, retrievals are also performed by using the SA method in parallel with the LS method. The SA method uses the same weights P_2, P_3, and P_4 as in (3.1), but the first weight has to be changed into

$$P_1 = 400\{\{|v_{\text{rob}}(t + \tau) - v_{\text{rob}}(t)|^2\}\}^{-1}, \quad (3.3)$$

because the first term (weighted by P_1) in the cost function for the SA method [see (3.4) of Xu et al. (1995)] is different from that in (2.2) for the LS method. Here a factor of 400 is chosen in (3.3) to make the averaged relative magnitude of P_1 (with respect to the remaining three weights) close to the relative magnitude of P_1 used by Xu et al. (1995). The relative magnitudes for the remaining three weights (with respect to each other) are in the ranges as suggested by Xu et al. (1995). A series of test experiments are performed (not shown) to compare the above weight selections for the SA method with those in Xu et al. (1995), and it is found that the time-dependent weight P_1 in (3.3) can slightly improve the retrievals, but the case-dependent weights P_2 and P_3 in (3.1) make the retrievals slightly worse.

As explained in Xu and Qiu (1994), because the data contain errors, the retrieval may be improved before a certain large number of iterations (around 120–250 steps for the SA method with the current microburst data) and then degrade slightly as the cost function further decreases toward the minimum. Thus, a fixed number of iterations (185 steps) was chosen in Xu et al. (1995). The minimization procedure used in this paper with (2.6) is more rational than a fixed number of iterations, but the retrievals become slightly worse than those in Xu et al. (1995). Because of this and the above weight selections, the SA retrievals in experiment 1 (see Table 1) are slightly worse than those in Xu et al. (1995) (see their Table 1). [Note that the retrieved radial winds were very close to the observed. The rms difference for the vector winds in Xu et al. (1995) can be directly compared with the rms difference for the tangential winds in this paper.]

4. Results of experiments

The averaged rms, RRD, and SCC for each group of 25 (or 12) retrievals in the experiments 1–5 (or 6) are summarized in Table 1. The groups are divided for the two methods (LS and SA) and two datasets (from FL-2 radar and UND radar). The averaged number of iterations is also listed for each group (see the columns under NI). In experiment 1, the LS method not only produces better retrievals but also takes fewer number of iterations to converge. Since one step of iteration in the LS method costs only about one-ninth of the CPU time for one step of iteration in the SA method, the LS method is much more efficient than the SA method. Among the 25 LS retrievals, the best (rms = 1.90 m s^{-1}) and worst (rms = 5.09 m s^{-1}) retrievals are shown and compared with the dual-Doppler observations in Figs. 2a–d and Figs. 3a–d, respectively. As shown, the gross patterns of the radial winds and vector winds are well retrieved in both cases, and many detailed features are captured by the retrieved field in Figs. 2c,d. As the retrieved wind fields are constrained by the smoothing operators [see the last two terms in (2.2)], they are generally weaker and smoother than the dual-Doppler observed. Since the LS and SA meth-

TABLE 1. Summary of the results (each averaged over 25 or 12 retrievals) for the six experiments. Here the root-mean-square (rms) difference, the relative rms difference (RRD), and the spatial correlation coefficient (SCC) are defined in Eqs. (3.2a)–(3.2c), and NI is the averaged number of iterations.

	FL-2 data				UND data			
Experiment number description	rms ($m\ s^{-1}$)	RRD	SCC	NI	rms ($m\ s^{-1}$)	RRD	SCC	NI
1. Control case (LS)	2.71	0.528	0.868	151	4.13	0.643	0.639	161
(SA)	3.04	0.579	0.837	300	4.39	0.680	0.609	218
2. Not retrieve mean forcing	3.15	0.592	0.810	112	4.22	0.661	0.604	147
	4.20	0.764	0.624	294	5.22	0.816	0.459	165
3. $P_3 = P_4 = 0$	13.42	2.617	0.374	232	16.12	2.536	0.336	205
	7.30	1.396	0.326	403	7.10	1.105	0.124	301
4. $\tau = 3\Delta\tau$ with $\Delta\tau = 60$ s	2.92	0.572	0.844	168	4.45	0.685	0.586	172
	3.21	0.610	0.810	249	4.75	0.717	0.577	185
5. $\tau = 5\Delta\tau$ with $\Delta\tau = 60$ s	2.58	0.540	0.880	144	3.89	0.605	0.659	159
	2.88	0.552	0.830	321	4.03	0.623	0.588	208
6. $\tau = 2\Delta\tau$ with $\Delta\tau = 120$ s	3.55	0.665	0.733	233	4.99	0.767	0.463	218
	3.41	0.639	0.740	229	4.34	0.661	0.459	225

ods use the same smoothing constraints [see (2.2) of this paper and (3.4) of Xu et al. (1995)], the LS retrievals and SA retrievals undergo about the same degree of smoothing.

Experiment 2 does not retrieve the time-mean forcing term F_m, and this deteriorates the SA retrievals more than the LS retrievals as shown in Table 1. The reason is that the LS method uses the model's equation (2.1) in a form of weak constraint and thus can tolerate equation error more than the SA method. When (2.1) is used as a strong constraint in the SA method, the equation error due to the neglected time-mean forcing term will accumulate during the time integration of the equation. This type of accumulation of equation error does not occur in the LS method because the time derivative term in the cost function is computed directly from the observed radial winds [see (2.2) and (2.3)].

Experiment 3 does not use the weak divergence constraint and weak vorticity constraint. Consequently the retrievals become very noisy, especially for the LS method. Without these smoothness constraints, the LS retrieval at a grid point is determined solely by its neighborhood gridpoint data, while the SA retrieval at a grid point is affected by the entire grid data. Thus, the LS retrievals are more sensitive to data noise than the SA retrievals. This explains why the LS method so critically depends on the smoothness constraints.

Experiment 4 (or 5) uses one more (or one less) time level of observation and thus a longer (or shorter) retrieving period τ than the control experiment. As shown in Table 1, using a few more time levels of data can increase the accuracy of the retrieval. However, as explained in Qiu and Xu (1992), if too many levels of observations are used, then the retrieving period τ will be too long and the quasi-steady assumption will be violated. In this case (not shown), the retrieved time-mean winds deteriorate due to the increased error of the averaged equation and the reduced temporal resolution.

Experiment 6 shows that the retrievals will become worse, especially for the LS method, if the time interval between two consecutive observations (i.e., time elapsed for one radar scan) is doubled. In this case, the SA method is superior to the LS method. Since the time derivative term in the cost function is computed directly from the observed radial winds, the LS method requires a relatively high temporal data resolution (obtained from rapid radar scans).

The above results also show that the retrievals from UND radar are statistically less accurate than those from FL-2 radar (see Table 1). Factors causing this statistical difference were diagnosed by Xu et al. (1994a, 1995) in terms of equation error and data error. In particular, it was found that the data error were relatively large and the mean advection term was relatively small for the SA retrievals from UND radar. These diagnostic results remain generally true here for the LS retrievals. The relatively small mean advection term for the UND radial winds can be further related to the fact that the wind vectors were largely tangential to the UND radar beams, while the large data error for the UND radial winds can be further related to the fact that the UND radar was farther distant from the retrieval domain, while the beamwidth and range-gate

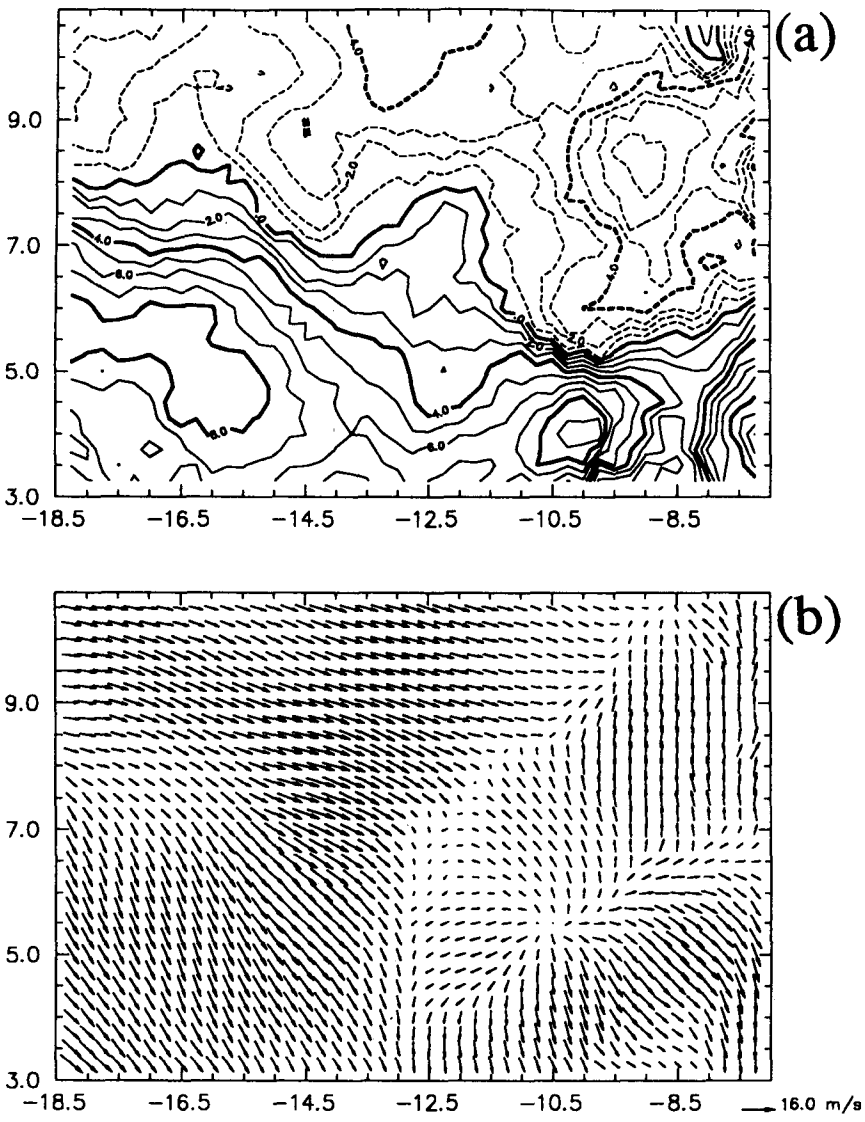

FIG. 2. Results of the one (of 50) run in experiment 1, which produced the best least squares (LS) retrieval from the FL-2 radar data. This run used five consecutive time levels of FL-2 radial wind data from 2213 to 2217 UTC 11 July 1988. (a), (b) The dual-Doppler analysis using both FL-2 and UND radar data for the microburst occurring during this time interval (2213–2217 UTC). (b) The two-dimensional time-mean wind field for the dual-Doppler analysis; (a) the tangential component of the time-mean wind as viewed from the position of FL-2. (d) Two-dimensional time-mean wind field retrieved from the FL-2 single-Doppler wind data by using the LS method; (c) the tangential component of the retrieved time–mean wind. The data shown are 190 m above the FL-2 radar (317 m above the UND radar). The length of a vector 16 m s^{-1} long is shown at the lower right of (b) and (c). The coordinate system is the same as in Fig. 1. The root-mean-square difference is rms = 1.90 m s^{-1}, and the spatial correlation coefficient is SCC = 0.91.

spacing for UND radar were about twice of those of FL-2 radar.

In addition to the above factors, the retrievals are also affected by the flow structures that yield different patterns in the radial wind fields viewed from the two radars. In general, as explained in Qiu and Xu (1992) and Xu et al. (1994a), the retrieval tends to be more (or less) accurate when the observed "tracer" (reflectivity or radial wind) field contains more (or less) significant spatial structures associated with larger (or smaller) spatial gradients. Note that Fig. 2a can be viewed approximately as the UND radial wind, while Fig. 3a can be viewed approximately as the FL-2 radial wind. Thus, although the radial wind fields are not

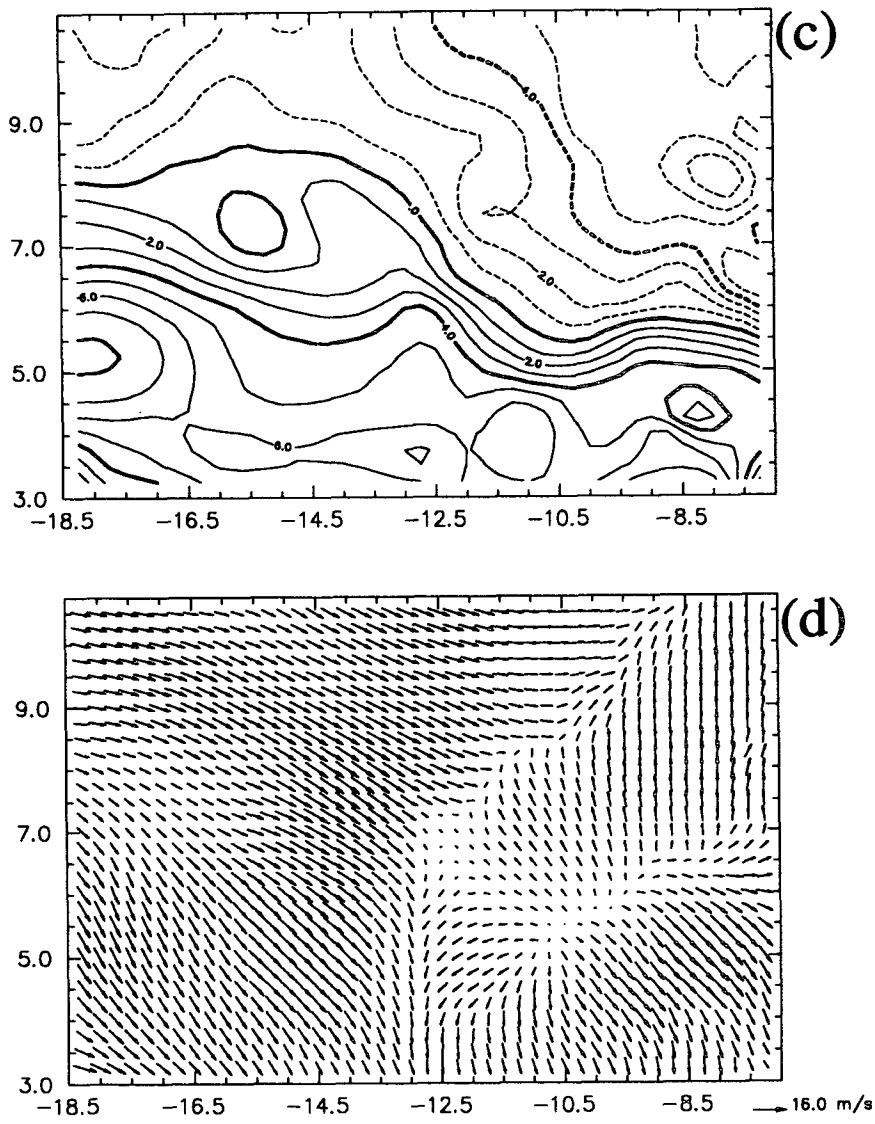

FIG. 2. (*Continued*)

shown, different patterns in the radial wind fields can be perceived from Figs. 2a and 3a and used to explain their impacts on the respective retrievals in Figs. 3c,d and 2c,d.

5. Sensitivities and weight selections

As we have seen from the experiments in the previous section, the weak divergence constraint and weak vorticity constraint (or other forms of smoothness constraints) are necessary and critical for suppressing the noise caused by data and equation errors. A question is then raised regarding how to objectively and optimally select their weights with respect to each other and with respect to the other weights. This problem is examined in this section together with the sensitivities of the retrievals to the weights.

In the control experiment, the four weights are selected as in (3.1), and these weights are now taken as the reference values and denoted by P_i^0 ($i = 1, 2, 3, 4$). With the remaining three weights fixed, we can change the first weight from its reference value P_1^0 to $P_1 = 2^n P_1^0$, where n is an integer ranging from -3 to 3. Retrievals are performed with these seven different settings of P_1, and the averaged (for 25 fields) rms differences between the retrieved and dual-Doppler observed tangential winds are plotted in Fig. 4 for the FL-2 radar data and in Fig. 5 for the UND radar data, where the solid curves denoted by v_α(LS) are for the LS method and the dot–dashed curves denoted by v_α(SA)

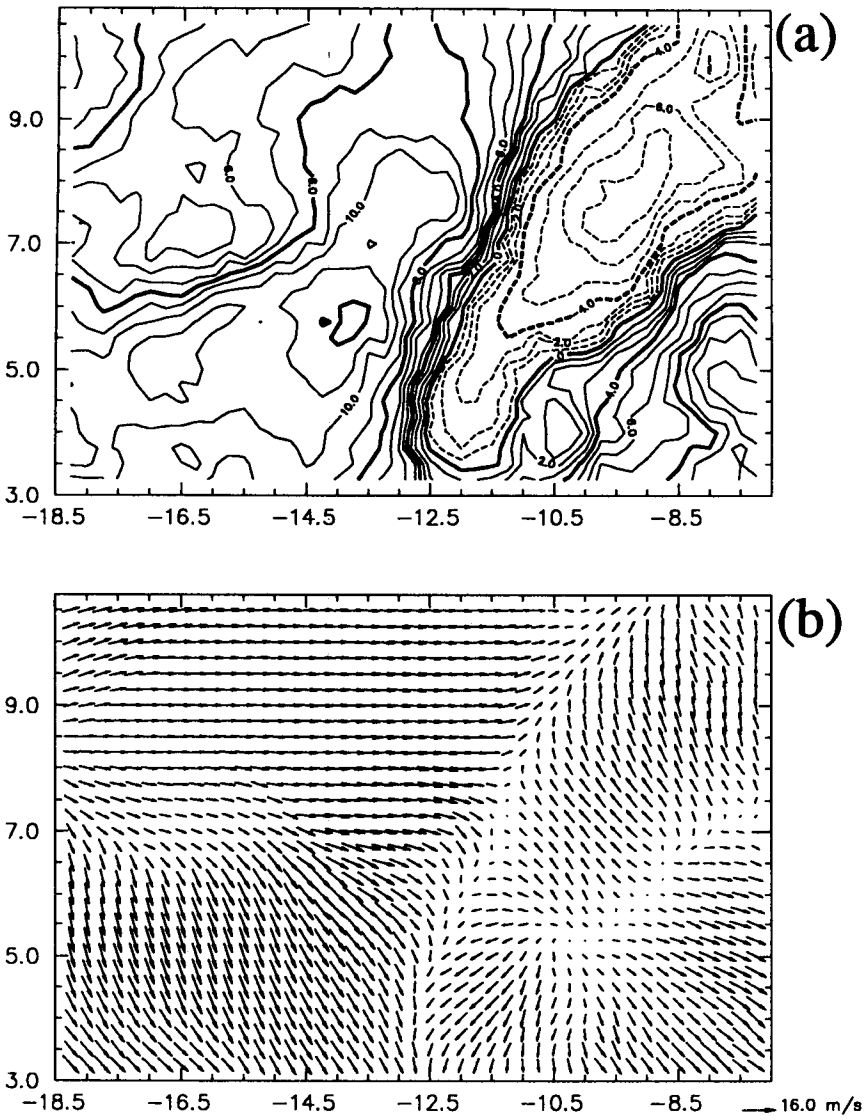

FIG. 3. As in Fig. 2 but for the one (of 50) run in experiment 1, which produced the worst LS retrieval from the UND radar data. This run used five consecutive time levels of UND radial wind data from 2217 to 2221 UTC 11 July 1988. The dual-Doppler analysis using both FL-2 and UND radar data for the microburst occurring during this time interval (2217–2221 UTC). The tangential winds in (a) and (c) are relative to the UND radar. The root-mean-square difference is rms = 5.09 m s^{-1}, and the spatial correlation coefficient is SCC = 0.74.

are for the SA method. As shown, when P_1 is increased (or decreased) by $2^3 = 8$ times, the rms difference increases by about 0.5 m s^{-1} for the LS retrievals and by about 0.2 m s^{-1} for the SA retrievals. Thus, for the averaged results, the LS retrievals are not very sensitive to the variation of P_1, while the SA retrievals are even less sensitive.

An individual retrieval may have a somewhat different sensitivity to the change of P_1. An example is shown in Fig. 6, where the LS retrieval (from the FL-2 radar data covering the period of 2211–2215) is slightly worse than the SA retrieval, and both retrievals are not sensitive to the decrease of P_1 (from P_1^0 down to $P_1^0/8$) but quite sensitive to the increase of P_1 (from P_1^0 up to $8P_1^0$).

Retrievals are also performed with $P_2 = 0$ for the above seven different settings of P_1. The rms differences between the LS retrieved and dual-Doppler observed tangential winds are plotted in Figs. 4–6 [see the dashed curves denoted by v_a(LS, $P_2 = 0$)]. As shown, the retrieved tangential winds become slightly worse when $P_2 = 0$. The rms differences between the

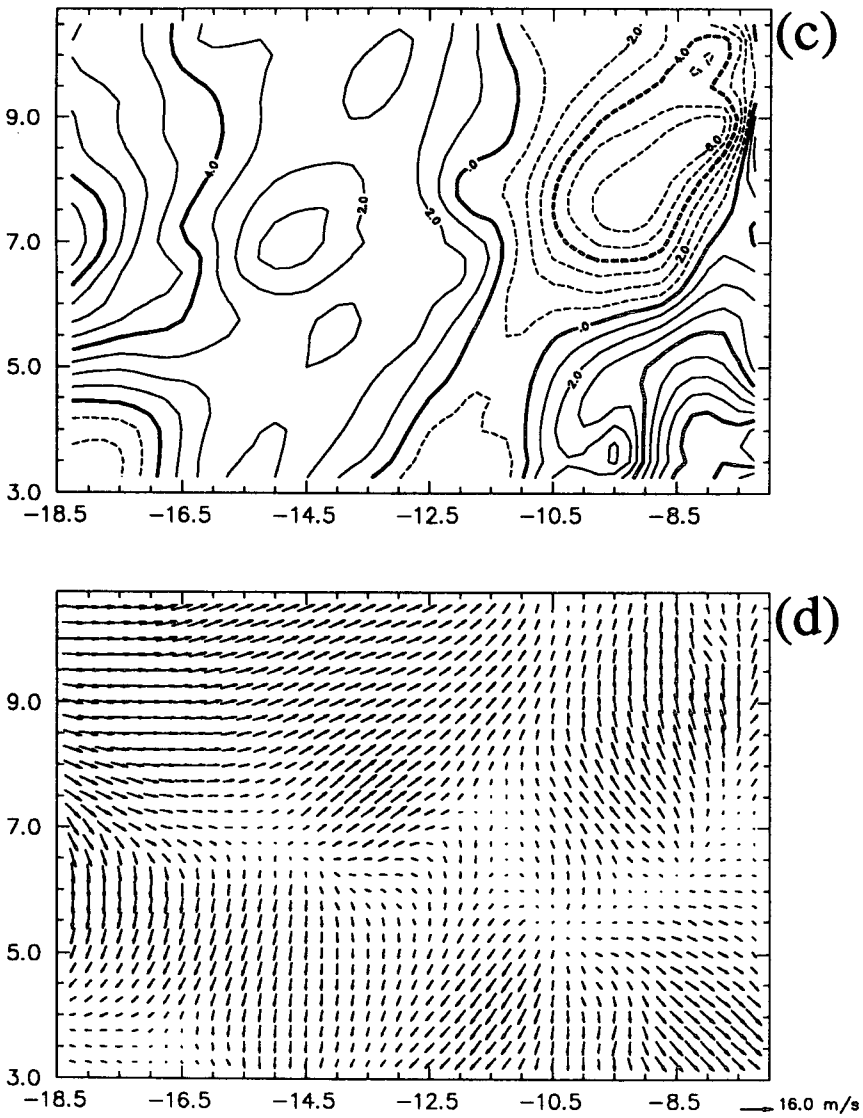

FIG. 3. (*Continued*)

LS retrieved and single-Doppler observed radial winds are also plotted in Figs. 4–6 [see the dotted curves denoted by v_r(LS, $P_2 = 0$)]. Note that with $P_2 = 0$ the averaged rms differences for v_r and for v_α have similar dependences on P_1/P_1^0, and, in particular, they both reach their respective minimums in the vicinity of $P_1/P_1^0 = 1$. This suggests that the optimal value for P_1 that minimizes the averaged rms difference for v_α can be estimated by the value for P_1 that minimizes the averaged rms difference for v_r. Since the latter value can be determined from single-Doppler data, the optimal value for P_1 (relative to P_3 and P_4) can be objectively estimated.

The above objective selection of P_1 work well for the averaged results but may not work well for every individual retrieval. For example, the result in Fig. 6 shows that the rms difference for v_r reaches the minimum at $P_1/P_1^0 = 4$, while the rms difference for v_α reaches the minimum at $P_1/P_1^0 = 1/2$. If $P_1/P_1^0 = 4$ is used to replace $P_1/P_1^0 = 1$, then the rms difference for v_α will increase from 2.32 to 2.87 m s^{-1} for this individual retrieval. To show the statistics, we denote by n_r (or n_α) the integer n in $P_1 = 2^n P_1^0$ that minimizes the rms difference for v_r (or v_α). As listed in Table 2, among the 50 LS retrievals (25 from FL-2 data and 25 from UND data), only 40% of the retrievals are in the range of $|n_r - n_\alpha| \leq 1$, while 64% of the retrievals are in the range of $|n_r - n_\alpha| \leq 2$. When $n = n_r$ is selected for each individual retrieval, the averaged rms difference for v_α is increased by 0.33 m s^{-1}, compared with

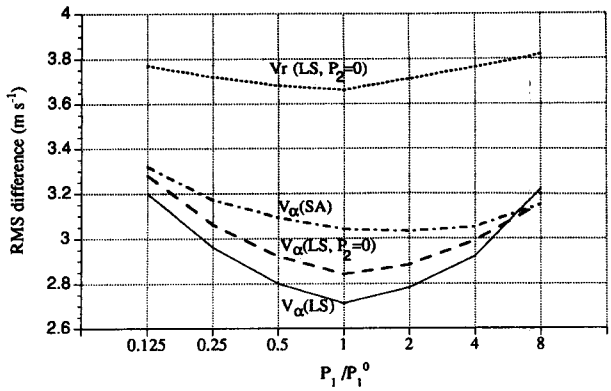

FIG. 4. Averaged rms differences versus P_1/P_1^0 for 25 retrievals from FL-2 radar data. The solid curve denoted by v_α(LS) is the rms difference for the tangential wind retrieved by the LS method with P_2, P_3, and P_4 given by Eq. (3.1). The dot–dashed curve denoted by v_α(SA) is the rms difference for the tangential wind retrieved by the SA method with P_2, P_3, and P_4 given by Eq. (3.1). The dashed curve denoted by v_α(LS, $P_2 = 0$) is the rms difference for the tangential wind retrieved by the LS method with P_3 and P_4 given by Eq. (3.1) but $P_2 = 0$. The dotted curve denoted by v_r (LS, $P_2 = 0$) is the rms difference for the radial wind retrieved by the LS method with P_3 and P_4 given by Eq. (3.1) but $P_2 = 0$.

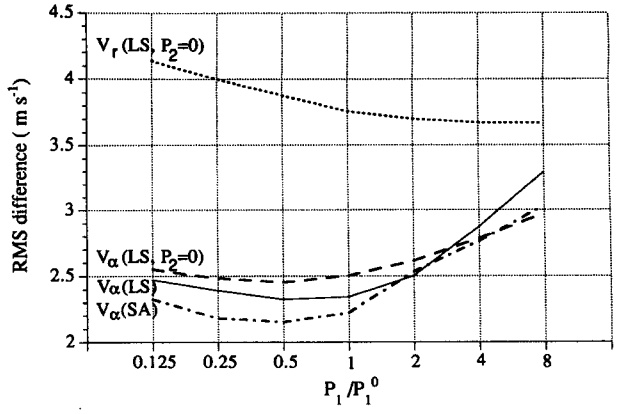

FIG. 6. As in Fig. 4 but for individual retrievals from FL-2 radar data over the period of 2211–2215 UTC.

the result obtained with $P_1/P_1^0 = 1$ (which is optimal for the averaged retrievals). Since this causes only a 10% increase of the rms difference, the above objective selection of P_1 may be still useful for an individual retrieval if only one or a few retrievals can be performed due to the availability of data for a concerned case.

As explained in section 3, ideally the weights P_3 and P_4 should be inversely proportional to the mean square amplitudes of the time-mean divergence and vorticity, respectively. With single-Doppler data, however, σ_d^2 and σ_ζ^2 can only be roughly estimated by the partial divergence and partial vorticity computed from the radial winds, and their estimated values in (3.1) are not optimal, especially for the UND data. Thus, it is necessary to examine the sensitivities of the retrievals to the variation of P_3 with respect to P_4. For this purpose, we set $P_3 = k_d P_3^0$ and $P_4 = k_\zeta P_4^0$ with a fixed sum of $k_d + k_\zeta = 2$ and variable k_ζ/k_d from 0.5 to 8, where P_3^0 and P_4^0 denote their respective reference values in (3.1). With the remaining two weights fixed, LS retrievals are performed for nine different settings of $k_\zeta/k_d = 0.5, 1, 2, 3, \cdots, 8$, and the averaged rms differences are plotted in Fig. 7. As shown, the reference setting of $k_\zeta/k_d = 1$ is not optimal, especially for the UND data. Note also that the optimal value for k_ζ/k_d that minimizes the rms difference for v_α is very close to the value for k_ζ/k_d that minimizes the rms difference for v_r. As the latter value can be determined from single-Doppler data, it provides an objective estimate of the optimal value for k_ζ/k_d that minimizes the rms difference for v_α. When the above objective selection of k_ζ/k_d applies to each individual retrieval, the averaged rms difference for v_α is increased only by 0.02 m s^{-1} for the FL-2 data and by 0.01 m s^{-1} for the UND data, compared with the result obtained with $k_\zeta/k_d = 1$. Thus, the above objective selection of k_ζ/k_d seems also suitable for an individual retrieval.

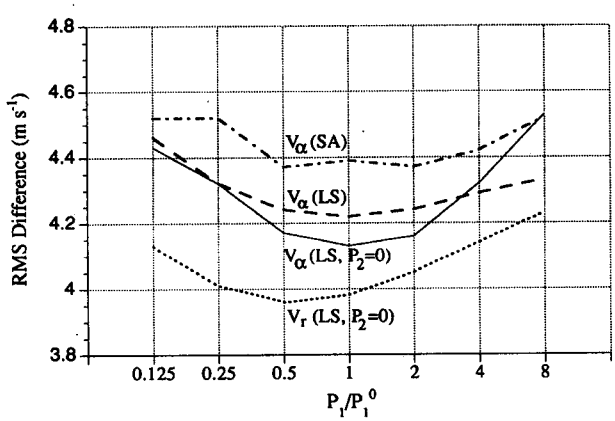

FIG. 5. As in Fig. 4 but for 25 retrievals from UND radar data.

6. Conclusions

In this paper, an LS method is developed for retrieving the low-altitude winds from single-Doppler scans. The method is tested with the Denver airport microburst data and compared with the SA method developed earlier by the authors. It is found that the LS

TABLE 2. Statistics for 50 LS retrievals grouped by different values of $|n_r - n_\alpha|$.

$\lvert n_r - n_\alpha \rvert$	0	1	2	3	4	5	6
Number of cases	9	11	12	10	3	4	1
Percent	18	22	24	20	6	8	2

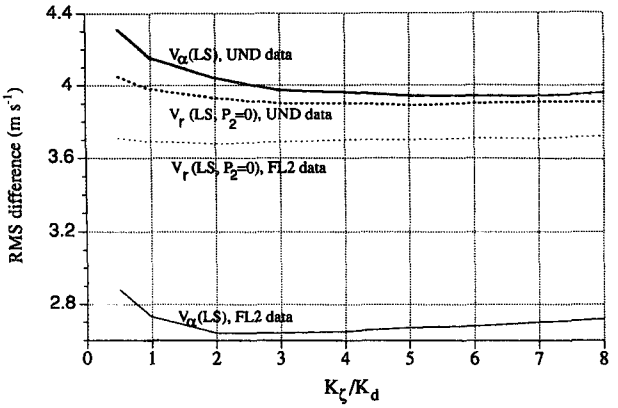

FIG. 7. Averaged rms differences versus k_ζ/k_d with $k_d + k_d = 2$ fixed for $P_3 = k_d P_3^0$ and $P_4 = k_\zeta P_4^0$. The thick curves are for retrievals from UND radar data, while the thin curves are for retrievals from FL-2 radar data. The solid curves denoted by v_α(LS) are for the tangential winds retrieved by the LS method with P_1 and P_2 given by Eq. (3.1). The dotted curves denoted by v_r(LS, $P_2 = 0$) is for the radial winds retrieved by the LS method with P_1 given by Eq. (3.1) but $P_2 = 0$.

method is slightly superior to the SA method for the microburst data obtained with fast radar scans ($\Delta\tau \approx 60$ s) but will become inferior to the SA method if the radar scanning period is prolonged ($\Delta\tau \approx 120$ s). The LS method uses the observed radial winds to compute the time-derivative term in the cost function [see (2.2)], so the retrieval is harmed by the finite-difference error when the temporal resolution is reduced. The SA method uses the observed radial winds to constrain the "predicted" winds obtained by integrating the radial momentum equation, so the retrieval is less sensitive to the temporal resolution but can be harmed by the error accumulated during the integration. This explains the relative advantages and disadvantages of each method.

Several detailed techniques previously developed for the SA method are applied to the LS method. These include (i) using multiple-time-level data to make the retrieval more accurate and less sensitive to the observational error; (ii) imposing smoothness constraints (such as the weak divergence and weak vorticity constraints) to suppress the noise caused by data and equation errors; (iii) retrieving the eddy coefficient and time-mean forcing term to improve the retrieval; (iv) using the observed radial wind to constrain the radial component of the retrieved time-mean wind. All these treatments are found significant in improving the LS retrievals. In comparison with the SA retrievals, however, the LS retrievals are more sensitive to data noise and thus depend more on the smoothness constraints. On the other hand, since the radial momentum equation is used as a weak constraint [see (2.1) and (2.2)], the LS method is computationally much more efficient than the SA method and can tolerate equation error more than the SA method or, perhaps, is less sensitive to equation error. The LS retrievals can be further improved (i) by using the previous time-level retrieval as the initial guess of the retrieval at the current time level and (ii) by incorporating the surface anemometer data into the method. These two detailed techniques can be applied to the LS method in the same way as in Xu et al. (1995) (though the details are not presented in this paper).

An effort is also made in this paper to find an objective way for weight selection. It is found that the optimal weights can be estimated from the statistical average of the weights that minimize the rms difference between the single-Doppler observed and retrieved time-mean radial winds. As in the SA method, the LS method has a high spatial resolution, reasonably good accuracy, and flexibility in using the other type of additional data. Moreover, the LS method is computationally much (10–20 times) more efficient than the SA method, and this makes the method very attractive for future operational uses (provided fast radar scans of data are available).

So far the SA and LA methods have been tested only with the Phoenix II radar data (Xu et al. 1994a,b) and the Terminal Doppler Weather Radar (TDWR) radar data (Xu et al. 1995). Since these data have relatively high resolutions ($\Delta\tau = 1$–2 min, $\Delta x = 100$–250 m) in time and space, it is not clear whether or which of the methods will be suitable for the NEXRAD data that have relatively coarse resolutions ($\Delta\tau = 4$–5 min, $\Delta x = 250$–1000 m). To address this problem, we tested the SA and LA methods with the same microburst data but the data resolutions are reduced to $\Delta\tau = 5$ min and $\Delta x = 1000$ m. Each time-mean wind field is retrieved from four time levels of data (that is, $\tau = 3\Delta\tau = 15$ min), and 15 retrievals are obtained from each radar and for each method. The averaged rms difference and SCC between the SA retrievals and dual-Doppler observations are rms = 4.2 m s^{-1} and SCC = 0.71 for the FL-2 data, and rms = 4.4 m s^{-1} and SCC = 0.66 for the UND data, which are significantly less accurate than those in Table 1. The LS retrievals have rms = 4.5 m s^{-1} and SCC = 0.43 for the FL-2 data, and rms = 5.0 m s^{-1} and SCC = 0.24 for the UND data, which are less accurate than the SA retrievals and much less accurate than those in Table 1. These results, though very preliminary, suggest some difficulties in retrieving microburst winds from NEXRAD-type single-Doppler data (especially when the temporal resolution becomes as coarse as 5 min). The SA and LA methods need to be further improved and tested with real NEXRAD data, and this should be the next step of study.

Acknowledgments. We are indebted to Marilyn Wolfson for her help with the Denver airport microburst data from the Massachusetts Institute of Technology Lincoln Laboratory. We are grateful to Robert Kropfli for his kind support with the Phoenix II data

from NOAA/ETL, which has been especially useful for the early development and tests of the method. We are thankful to Hongdao Gu, Jinxian Yu, and Jidong Gao for their assistance in many aspects and to Alan Shapiro, Richard Doviak, Peter Ray and anonymous reviewers for their comments and suggestions. We acknowledge the computational support provided by SCD/NCAR, and NCAR is sponsored by the National Science Foundation. This work is supported by NSF Grant ATM91-20009 at CAPS, the NOAA Contract NA37RJ0203, the U.S. Air Force Grant F49620-95-1-0320, and the NSF Grants ATM-9113906 at CIMMS, University of Oklahoma. The first author also acknowledges the support provided by the Chinese NSF Grant 49375241.

REFERENCES

Elmore, K. L., M. K. Politovich, and W. R. Sand, 1990: The 11 July 1988 Microburst at Stapleton International Airport, Denver, CO. Preprints, *16th Conf. on Severe Local Storms,* Kananaskis Park, Alberta, Canada, Amer. Meteor. Soc., 368–372.

Gal-Chen, T., and J. Zhang, 1993: On the optimal use of reflectivity and single-Doppler radar velocities to deduce 3-D motions. Preprints, *26th Int. Conf. on Radar Meteorology,* Norman, OK, Amer. Meteor. Soc., 414–416.

Kapitza, H., 1991: Numerical experiments with the adjoint of a non-hydrostatic mesoscale model. *Mon. Wea. Rev.,* **119,** 2993–3011.

Laroche, S., and I. Zawadzki, 1994: A variational analysis method for the retrieval of three-dimensional wind field from single-Doppler radar data. *J. Atmos. Sci.,* **51,** 2664–2682.

Liou, Y. C., T. Gal-Chen, and D. K. Lilly, 1991: Retrieval of wind temperature and pressure from single Doppler radar and a numerical model. *25th Int. Conf. on Radar Meteorology,* Paris, France, Amer. Meteor. Soc., 151–154.

Proctor, F. H., and R. L. Bowles, 1992: Three-dimensional simulation of the Denver 11 July 1988 microburst-producing storm. *Meteor. Atmos. Phys.,* **49,** 107–124.

Qiu, C., and Q. Xu, 1992: A simple adjoint method of wind analysis for single-Doppler data. *J. Atmos. Oceanic Technol.,* **9,** 588–598.

Sasaki, Y. K., 1970: Some basic formalisms in numerical variational analysis. *Mon. Wea. Rev.,* **98,** 875–883.

Shapiro, A., S. Ellis, and J. Shaw, 1995: Single-Doppler velocity retrievals with Phoenix II data: Clear air and microburst wind retrievals in the planetary boundary layer. *J. Atmos. Sci.,* **52,** 1265–1287.

Sun, J., and A. Crook, 1994: Wind and thermodynamic retrieval from single-Doppler measurements of a gust front observed during Phoenix II. *Mon. Wea. Rev.,* **128,** 1075–1091.

——, D. W. Flicker, and D. K. Lilly, 1991: Recovery of three-dimensional wind and temperature fields from single-Doppler radar data. *J. Atmos. Sci.,* **48,** 876–890.

Thacker, W. C., and R. B. Long, 1988: Fitting dynamics to data. *J. Geophys. Res.,* **93**(C2), 1227–1240.

Tuttle, J. D., and G. B. Foote, 1990: Determination of the boundary layer airflow from a single-Doppler radar. *J. Atmos. Oceanic Technol.,* **7,** 218–232.

Xu, Q., and C. Qiu, 1994: Simple adjoint methods for single-Doppler wind analysis with a strong constraint of mass conservation. *J. Atmos. Oceanic Technol.,* **11,** 289–298.

——, ——, and J. Yu, 1994a: Adjoint-method retrievals of low-altitude wind fields from single-Doppler reflectivity measured during Phoenix II. *J. Atmos. Oceanic Technol.,* **11,** 275–288.

——, ——, and ——, 1994b: Adjoint-method retrievals of low-altitude wind fields from single-Doppler wind data. *J. Atmos. Oceanic Technol.,* **11,** 579–585.

——, ——, H. Gu, and J. Yu, 1995: Simple adjoint retrievals of microburst winds from single-Doppler radar data. *Mon. Wea. Rev.,* **123,** 1822–1833.